ICAST2011 #050

# Panel Resonance Control and Cavity Control in Double-Panel Structures for Active Noise Reduction

Jen-Hsuan Ho[1], Arthur Berkhoff [1, 2]

[1]Department of Electrical Engineering, University of Twente, Drienerlolaan 5, P.O.Box 217
7500 AE Enschede, The Netherlands
[2]TNO, Acoustics Department, P.O. Box 155, 2600AD Delft, The Netherlands

**Abstract**

An analytical and experimental investigation of panel resonance control and cavity control in a double-panel structure is presented in this paper. The double-panel structure, which consists of two panels with air in the gap, is widely adopted in many applications such as aerospace due to its low weight and effective transmission-loss at high frequencies. However, the resonance of the cavity and the poor transmission-loss at low frequencies limit its noise control performance. In this paper, the resonance of the cavity and the panels are considered simultaneously to increase the noise transmission-loss. A structural-acoustic coupled model is developed to investigate the vibration of the two panels, the acoustic resonance in the air cavity, and the control performance. The control design can be optimized through the model using a combined stability analysis incorporating both structural and acoustic control. Finally, the results will be presented and discussed.

## 1. INTRODUCTION

The increasing need for a comfortable environment points to the importance of noise control technology. Passive control, which commonly means applying high damping materials and installing resonators in the system, can be effective in reducing the noise at high frequencies[1, 2]. However, passive control at low frequencies usually has much less noise reduction and comes with a heavy implementation because the acoustic wavelengths are much longer than the damping structure[3, 4]. On the other hand, with the development of smart materials and computational power, active noise control has received increasing attention in the last decades due to the possible advantages of reduced weight and better performance at low frequencies. Active noise control (ANC) has found successful applications in relatively small space regions with broadband noise control[5-7]. However, ANC is a 3D wave propagation problem; for a larger control space region, the implementation will become very complicated and inefficient. Acoustic structural active control (ASAC) can simplify a 3D problem to a 2D problem by directly control the vibrating structure to reduce its radiating sound pressure instead of dealing with 3D acoustic wave propagation. [6, 8]. Furthermore, for a large configuration, decentralized control or distributed control can make the controller suitable for more practical implementations[9-13]. Control methods also need to consider the additional weight of the installation[14]. With the advantage of a low weight structure, the double panel with an air gap structure is another common implementation for noise reduction [1, 15]. Due to their compact dimensions and fast response, piezoelectric materials have been investigated and applied frequently for vibration control of smart structures[5, 12, 16]. Decentralized feedback control strategy has been noted for its remarkable performance for the broadband objective [17].

In this paper, the characteristics of the double panel structure at resonance frequencies are analyzed. The structural control and the cavity control with feedback control were simulated to compare and derive the optimized control result. This paper is composed of four sections. First, the multiple fully coupled interaction control theory and the stability analysis method are introduced. Second, the finite element method model and the experiment measurement methods are described. Finally, the multiple feedback control results of the structure control, the cavity control and the combination control are shown and compared.

*Corresponding authors* e-mail: j.ho@utwente.nl, a.p.berkhoff@utwente.nl, arthur.berkhoff@tno.nl

## 2. MULTIPLE DECENTRALIZED CONTROL

### 2.1 Control loop

Fig. 1 illustrates the signal block diagram of a feedback control system. $\mathbf{G}(j\omega)$ is the plant response matrix, $\mathbf{H}(j\omega)$ is the controller matrix, $\mathbf{y}(j\omega)$ is the error signal matrix detected by the sensors, and $\mathbf{d}(j\omega)$ is the noise source signal matrix, which is the error signal without input control signals.

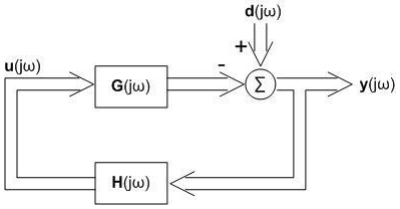


**Figure 1.** Direct velocity feedback systems.

From the block diagram above, $\mathbf{y}(j\omega)$ can be represented as Eq. (1)

$$\begin{aligned}\mathbf{y}(j\omega) &= \mathbf{d}(j\omega) - \mathbf{y}(j\omega)\cdot\mathbf{G}(j\omega)\mathbf{H}(j\omega) \\ \mathbf{y}(j\omega) &= (\mathbf{I} + \mathbf{G}(j\omega)\mathbf{H}(j\omega))^{-1}\cdot\mathbf{d}(j\omega)\end{aligned} \tag{1}$$

The physical interactions between each control unit in the realistic condition are presented with a multiple channel plant transfer matrix $\mathbf{G}(j\omega)$.

$$\mathbf{G}(j\omega) = \begin{bmatrix} \mathbf{G}_{11}(j\omega) & \cdots & \mathbf{G}_{1m}(j\omega) \\ \vdots & \ddots & \vdots \\ \mathbf{G}_{l1}(j\omega) & \cdots & \mathbf{G}_{lm}(j\omega) \end{bmatrix} \tag{2}$$

where $\mathbf{G}_{lm}(j\omega)$ is the response at the $l^{th}$ sensor under the input from the $m^{th}$ actuator without the disturbance source $\mathbf{d}(j\omega)$.

### 2.2 Control stability

The stability of a feedback control system can be unconditionally guaranteed when the sensors and the actuators are dual and collocated. Otherwise, the control gain will be limited. To determine the stability of MIMO decentralized control systems, the Nyquist criterion can be used. When the plot of Eq. (3) below neither crosses nor encircles the origin (0, 0), the system is stable[17].

$$\det[\mathbf{I} + \mathbf{G}(j\omega)\mathbf{H}(j\omega)] \tag{3}$$

However, the stable system can become unstable when there are perturbations. The ability of the system to withstand the perturbations are defined by stability margins. We use gain margin, phase margin, and modulus margin to determine the stability of the system.

## 3. MODEL ANALYSIS AND MEASUREMENT

### 3.1 Acoustic-structural interaction FEM model

The finite element method (FEM) is applied to analyze the characteristics of our system. To accurately estimate the system, the acoustic and structural properties need to be considered simultaneously. The relationship of the acoustic pressure in the fluid domain and the structural deformation in the solid domain are

linked as described below. In the solid domain, a normal force $\mathbf{F}_p$ is produced by the fluid pressure $p$ on the fluid-solid interacting boundaries,

$$\mathbf{F}_p = -\mathbf{n}_s p \tag{4}$$

In which $\mathbf{n}_s$ is the normal vector of the solid boundaries. In the acoustic fluid domain, the acceleration of the fluid-solid interacting boundaries can be derived from the acceleration $\mathbf{u}_{tt}$ of the structure,

$$a_n = \mathbf{n} \cdot \mathbf{u}_{tt} \tag{5}$$

With Eq. (4) and Eq. (5), the interaction between the acoustic field and the solid structure can be investigated.

The model consists of two simply supported panels and a cavity with 35mm thickness is used to analyze the resonant behavior and the sound transmission of a double panel. An incident spherical pressure wave from the corner of the bottom side, which can produce an asymmetric incident noise wave, presents the primary noise source (Fig. 2). The parameters used for the simulation model are given in Table 1. The acrylic box is modeled with a hard-wall boundary.

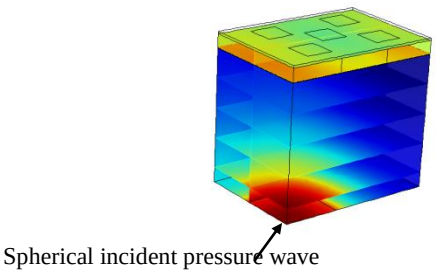


**Figure 2.** Acoustic-structure interaction model.

**Table 1.** Model parameters

| | Parameters | Values | unit |
|---|---|---|---|
| Aluminum panel | Dimensions | 420*297*1 | [$mm^3$] |
| | Density | 2700 | [$kg/m^3$] |
| | Young's modulus | 70 | [GPa] |
| | Poisson's ratio | 0.33 | |
| | Loss factor | 0.03 | |
| Honeycomb panel | Dimensions | 420*297*5.8 | [$mm^3$] |
| | Density | 409 | [$kg/m^3$] |
| | Young's modulus | 3.7 | [GPa] |
| | Poisson's ratio | 0.33 | |
| | Loss factor | 0.03 | |
| PZT patches | Dimensions | 7.24*7.24*0.264 | [$mm^3$] |
| | Density | 7800 | [$kg/m^3$] |
| | Young's modulus | 52 | [GPa] |
| | Poisson's ratio | 0.33 | |
| | Strain coefficient $d_{31}$ | -190 | [meter/Volt] |
| Acrylic box | Inner Dimensions | 420*297*350 | [$mm^3$] |
| | Wall thickness | 40 | [mm] |
| Middle cavity | Inner Dimensions | 420*297*35 | [$mm^3$] |

### 3.2 Piezoelectric actuators

Piezoelectric materials offer the advantages of fast response and compact dimensions. Laminar piezoelectric patches attached to a plate can be represented as four line moments on the edges of the piezoelectric patch[18] (Fig. 3). $E_p$ is the Young's modulus of the piezoelectric patch, $V$ is the controlling voltage applied to the patch, $d_{31}$ is the piezoelectric constant, $M_p$ is the moment per unit length. The piezoelectric control force is presented as these four line moments in our numerical analysis.

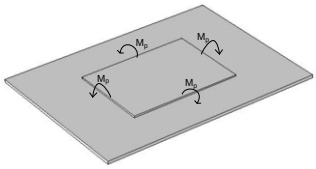

**Figure 3.** Equivalent piezoelectric loads.

$$M_p = -E_p d_{31} h V \tag{6}$$

### 3.3 Double panel with acrylic box

A double panel mounted on a rectangular box was set up for measurement. A loudspeaker in the bottom of the rectangular box generated the primary noise source. This box was made with 40 mm thick walls of acrylic plates to prevent the sound from leaking through side walls. The inner dimensions of the box were 420*297*350 $mm^3$. The primary noise source first entered an aluminum panel (the incident panel), then a layer of air of 35mm thickness followed by a honeycomb panel (the radiating panel). The transmitted sound of this double panel structure can be measured above the radiating panel (Fig. 4). Fig. 5 shows the positions of 5 pzt actuators and 5 velocity sensors on the radiating panel.

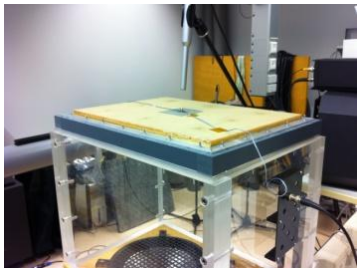

**Figure** 4. Experiment setup.

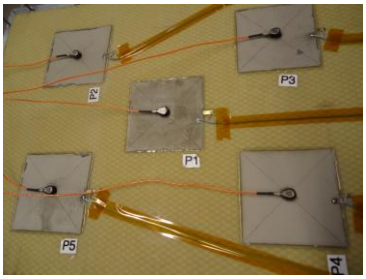


**Figure 5.** 5 pzt control sets on the radiating panel.

## 4. SIMULATION AND EXPERIMENT RESULTS

Structural control, cavity control, and combined control results will be compared numerically in this section.

### 4.1 Model validation

To validate the numerical analysis, a comparison of the kinetic energy response of a single panel for excitation with one piezoelectric patch between the simulation and the experiment is shown in Fig. 6. Nine accelerometers on the surface were used to measure the kinetic energy of the panel. To further validate the structural-acoustic interaction result, a double panel model and the experimental measurement are compared. In Fig. 7, the number of the resonant peaks increases because of the resonance contributions from the incident panel and the cavity. Fig. 6 shows that the numerical model can accurately present the practical sensor-actuator response in a single panel structure. Fig. 7 shows that the numerical model can present the practical sensor-actuator response in a double panel structure with reasonable accuracy.

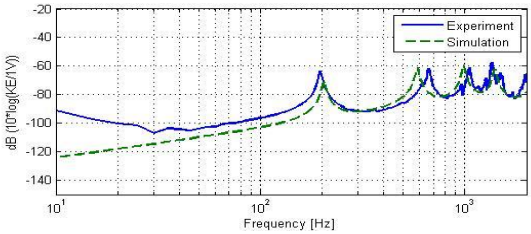


**Figure 6.** Kinetic energy of the single panel.

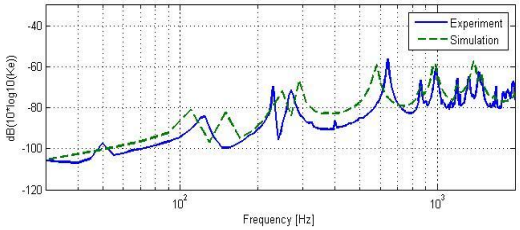


**Figure 7.** Kinetic energy of radiating panel in double panel structure.

## 4.2 Structural control

Pzt actuators are expected to have excellent control performance on smart structures and also are applied in active noise control. Therefore in a structural control design, piezoelectric patches are installed on the incident/radiating panel with velocity sensors located in collocated positions to control the vibration of the panel.

### 4.2.1 Numerical analysis

A configuration of ten control sets is shown in Fig. 8, where five control sets are on the incident panel (bottom panel) and five control sets are on the radiating panel (top panel). To ensure the stability of the structure control loop, the maximum control gain can be found by utilizing Nyquist analysis. Table 2. shows the response of a control gain of 500 for two cases, the left figure is applying the control sets on the incident panel and the right figure is applying control sets on the radiating panel. These plots do not encircle the origins which guarantee stability of the system.

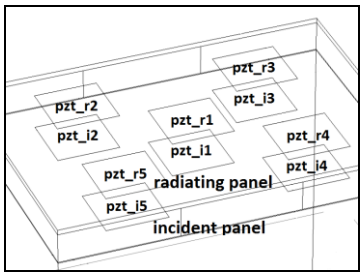


**Figure 8.** Control sets on the panels.

**Table 2.** Nyquist plot from 10-1000Hz

| Control sets position | On the incident panel | On the radiating panel |
|---|---|---|
| Nyquist plot | 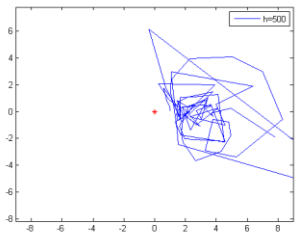 | 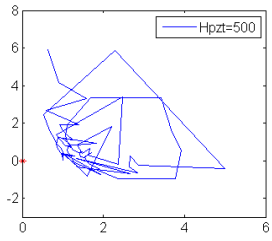 |

The control performances of various control positions are shown in Fig. 9. The reduction of double panel resonance with the pzt actuators located on the radiating panel is limited at the resonance frequencies of 80Hz, 140Hz, and 190Hz, while applying the pzt actuators on the incident panel can effectively reduce these resonant peaks. On the other hand, the peak at 330Hz has noticeable reductions with the pzt actuators on the radiating panel but on the incident panel. To further analyze the effect difference, the resonant mode shapes of the radiating panel are plotted (Table 3). The resonance frequencies of 80Hz, 140Hz, and 190Hz come from the resonant modes of the incident panel, and these resonant peaks can be effectively reduced by the incident-panel pzt actuators. Inversely, the resonance frequency of 330Hz comes from the radiating panel and it can be well controlled by the radiating-panel pzt actuators. These resonant peaks can be reduced when both of the radiating panel and the incident panel are under control. Therefore, to ensure the performance of the structural control, the control sets should be applied to those panels with the dominated resonant modes. The resonance frequency of 440Hz is the resonance frequency of the noise source (the source cavity).

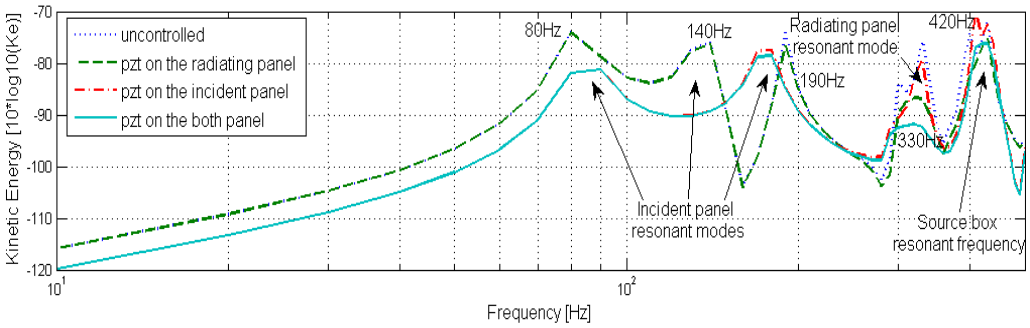


**Figure 9.** Kinetic energy of the radiating panel.

**Table 3.** Mode shapes of the radiating panel.

| Frequency [Hz] | 80 | 140 | 190 | 330 | 420 |
|---|---|---|---|---|---|
| Uncontrolled | 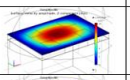 | 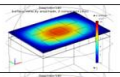 | 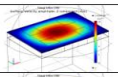 | 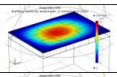 | 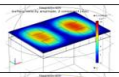 |
| pzt on the radiating panel | 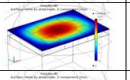 | 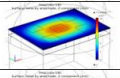 | 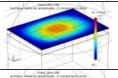 | 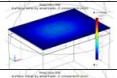 | 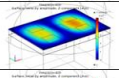 |
| pzt on the incident panel | 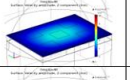 | 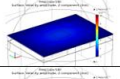 | 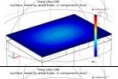 | 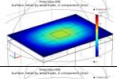 | 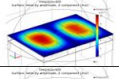 |
| pzt on both panels | 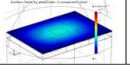 | 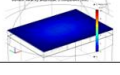 | 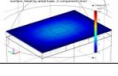 | 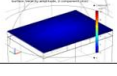 | 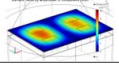 |

### 4.2.2 Real time feedback control experimental results

The resonance frequencies of a single panel structure are dominated by this single panel. However, the resonance frequencies of a double panel structure come from both the resonant modes of the incident panel and the radiating panel. To compare the control effect of pzt actuators on a single panel structure and a double panel structure, a single pzt actuator and a velocity sensor were installed on the centre of the radiating panel surface. The difference between these two measurements is, in the single panel structure, the radiating panel directly receives the incident noise whereas in the double panel structure, the noise source first passes through an incident panel and a cavity. The experiment results in Fig. 10 and Fig. 11 show that pzt actuators on the radiating panel only ensure a significant influence on the vibration level of the single panel structure, where the resonance is dominated by the controlled panel. Since only a single central pzt patch is used, only the mode with lowest resonance frequency can be controlled. In the double panel structure, almost no reduction of the vibration level can be noticed because the first few peaks are not dominated by the controlled panel.

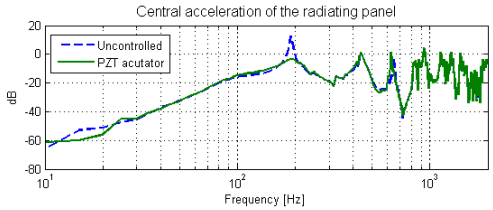


**Figure 10.** Single panel structure.

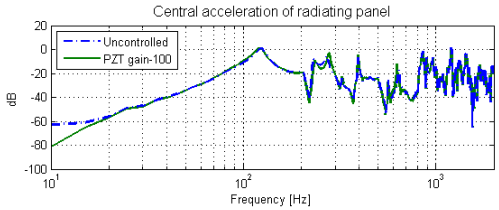


**Figure 11.** Double panel structure.

### 4.3 Cavity control

In the double panel structure, the resonance from the cavity dominates considerably resonant energy as well. To reduce the resonance in the cavity, six decentralized controllers were installed in the middle cavity between these double panels. Each controller detects sound pressure with one microphone and produces a secondary source by one loudspeaker from the side of the cavity. Two types of loudspeaker sources, which are pressure source and acceleration source, are analyzed. The distribution of these six control sets is shown in Fig12.

The influence from the actuators on each sensor is considered simultaneously to derive the total plant transfer function $\mathbf{G}(j\omega)$. From the Nyquist plot of $\det[\mathbf{I}+\mathbf{G}(j\omega)\mathbf{H}(j\omega)]$ shown in Table 4, the response does not pass through the origin. It shows the system is stable with constant feedback control gain.

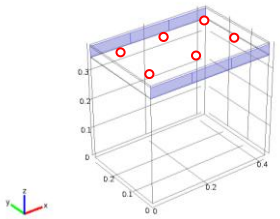

**Figure 12.** Control sets distribution.

**Table 4.** Nyquist plot from 10-1000Hz

| Source type | Pressure source | Accleration source |
|---|---|---|
| Nyquist plot | 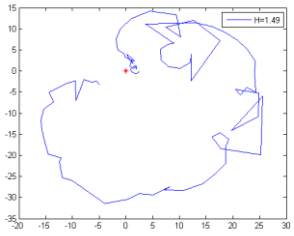 | 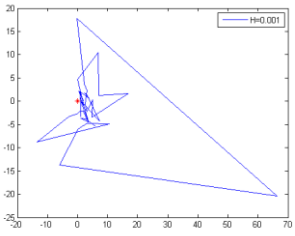 |

The cavity control result of these two loudspeaker sources is compared in Fig. 13, where a pressure source loudspeaker leads to better noise reduction. In a realistic control system, the most common type of loudspeaker, called a dynamic loudspeaker, can be assumed to operate as acceleration source above the resonance frequency. To implement a pressure source loudspeaker in practice, a pressure source actuator design is required.

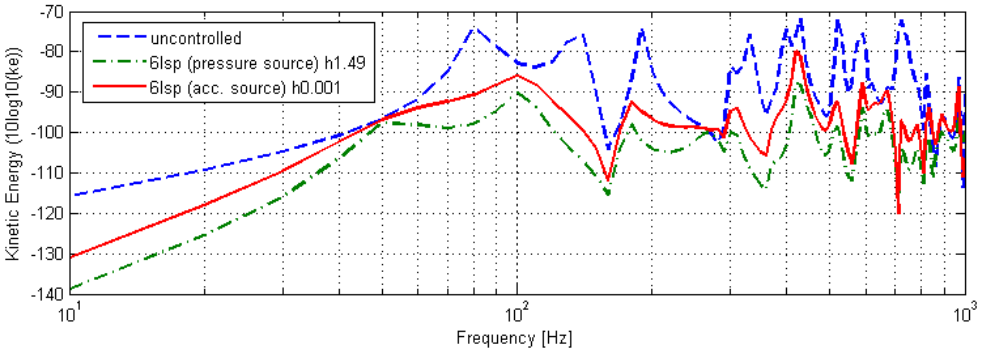


**Figure 13.** Control effect of cavity control**.**

### 4.4 Combined control

The stability of cavity control (loudspeaker and microphone combinations) and structural control (piezoelectric actuators and velocity sensors) can be analyzed using the fully coupled plant transfer function in which the maximum 16 actuators and 16 sensors are considered simultaneously. Fig. 14 shows the full model with all the control sets. Based on equal gain margin, phase margin, and modulus margin (Table 5), the effects of various control strategies are compared. The frequency responses of the control effect are shown in Fig. 15, which indicates that the use of pressure source loudspeakers leads to excellent noise reduction.

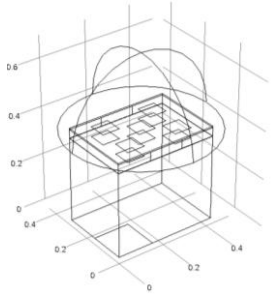

**Figure 14.** Full model with all the control sets.

**Table 5.** Stability margins of different control strategies.

| Combinations | Control gain | Gain margin | Phase margin | Modulus margin |
|---|---|---|---|---|
| 6 loudspeakers acc. source | 0.001 | Inf. | -85.4° | 1.018 |
| 6 loudspeakers pressure source | 1.49 | Inf. | -85.0 ° | 1.020 |
| 10 pzt (inc. & rad. panels) | 195 (inc.) 205 (rad.) | Inf. | -85.1 ° | 1.001 |
| 6 acc. loudspeakers & 10 pzt | 0.0002 (lsp) 130 (pzt) | Inf. | -85.2 ° | 1.013 |

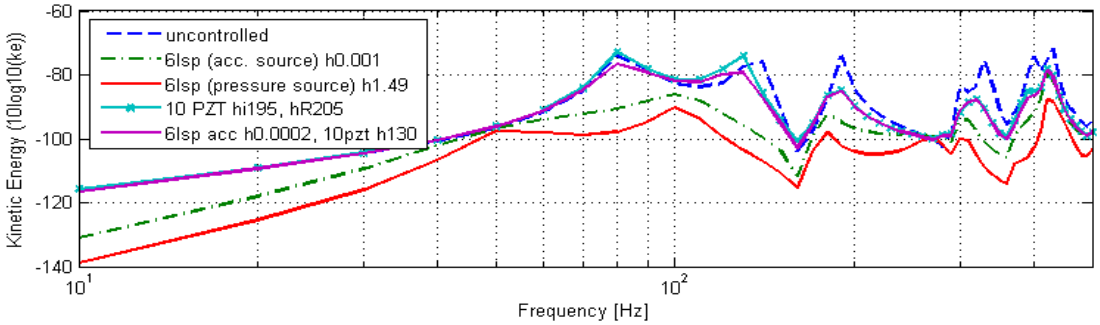


**Figure 15.** Comparison of different control strategies.

## 5. CONCLUSIONS

This paper has shown that although radiating-panel pzt actuators can effectively reduce the noise from a single panel structure, pzt actuators should be simultaneously applied to both the incident panel and the radiating panel in a double panel structure where the panels are simply supported. This is because the resonance frequencies of a double panel structure are dominated by both the incident panel and the radiating panel. Piezoelectric actuators can effectively reduce the noise when they are attached to the dominant resonant panel.

To further improve the control effect, a combination with cavity control can improve the performance. Based on same control stability margins, a pressure source loudspeaker leads to excellent noise reduction in the numerical analysis. To practically implement it, a pressure source actuator design is required.

## ACKNOWLEGEMENTS

This research and development is funded by STW, project IMPEDANCE (Integrated Modules for Power Efficient Distributed Active Noise Cancelling Electronics). The experimental development has been supported by Henny Kuipers and Geert Jan Laanstra of Signals and Systems group, Faculty of EEMCS, University of Twente.

## REFERENCES

1. M. Qibo and S. Pietrzko, 2010, "Experimental study for control of sound transmission through double glazed window using optimally tuned Helmholtz resonators," *Applied Acoustics,* 71, pp. 32-8.
2. C. Hirunyapruk, *et al.*, 2010, "A tunable magneto-rheological fluid-filled beam-like vibration absorber," *Smart Materials and Structures,* **19**, p. 055020 (10 pp.).
3. F. Fahy and J. Walker, 1998, *Fundamentals of Noise and Vibration*, Routledge, UK.
4. F. Fahy and P. Gardonio, 2007, *Sound and structural vibration: radiation, transmission and response* 2ed Edition, Academic Press, Elsevier, London.
5. O.E. Kaiser, S.J. Pietrzko,M.Morari, 2003, "Feedback control of sound transmission through a double glazed window", *Journal of Sound and Vibration* **263** 775–795.
6. J. Pan, C. Bao, 1998, "Analytical study of different approaches for active control of sound transmission through double walls", *Journal of the Acoustical Society of America* **103** (2) 1916–1922.
7. S. Pietrzko, O. Kaiser, 1999, "Experiments on active control of air-borne sound transmission through a double wall cavity", *Proceeding of International Symposium on Active Control of Sound and Vibration*, Florida, pp. 355–362.
8. J.P. Carneal, C.R. Fuller, 2004, "An analytical and experimental investigation of active structural acoustic control of noise transmission through double panel systems", *Journal of Sound and Vibration* **272** 749–771.
9. P. Gardonio, *et al.*, 2004, "Smart panel with multiple decentralized units for the control of sound transmission. Part I: theoretical predictions," *Journal of Sound and Vibration* **274**, pp. 163-92.
10. P. Gardonio, *et al.*, 2004, "Smart panel with multiple decentralized units for the control of sound transmission. Part II: design of the decentralized control units," *Journal of Sound and Vibration,* **274**, pp. 193-213.
11. P. Gardonio, *et al.*, 2004, "Smart panel with multiple decentralized units for the control of sound transmission. Part III: control system implementation," *Journal of Sound and Vibration,* **274**, pp. 215-32.
12. A. P. Berkhoff and J. M. Wesselink, 2009, "Combined MIMO adaptive and decentralized controllers for broadband active noise and vibration control", *Proceeding of International Symposium on Active Control of Sound and Vibration*, Ottawa, Canada, pp. 1-12.
13. P. A. Nelson and S. J. Elliott, 1992, *Active Control of Sound*, 1st Edition, Academic Press, London.
14. A. P. Berkhoff, 2004, "Weight reduction and transmission loss tradeoffs for active/passive panels with

miniaturized electronics," *Proceeding of International Symposium on Active Control of Sound and Vibration*, Washington DC, USA, pp. 1-12.

15. N. Alujevic, *et al.*, 2008, "Smart double panel with decentralized active dampers for sound transmission control," *AIAA Journal*, **46**, pp. 1463-75.
16. A. P. Berkhoff, 2001, "Piezoelectric sensor configuration for active structural acoustic control," *Journal of Sound and Vibration*, **246**, pp. 175-83.
17. S. J. Elliott, *et al.*, 2002, "Active vibroacoustic control with multiple local feedback loops," *Journal of the Acoustical Society of America*, **111**, pp. 908-15.
18. A. Preumont, 2004, *Vibration control of active structures*, 2ed Edition, Kluwer Academic Publishers, New York.